# Effect of heating rate on microstructure and electrical properties of microwave sintered $CaCu_3Ti_4O_{12}$ ceramics

Sandeep Kumar[1], Neetu Ahlawat[1]*, Navneet Ahlawat[2]

[1]*Department of Applied Physics, Guru Jambheshwar University of Science and Technology, Hisar, Haryana 125001, India*
[2]*Matu Ram Institute of Engineering and Management, Rohtak, Haryana 124001, India*

*Corresponding author. Tel: (+91) 1662-263389; Fax: ( +91) 1662-276240, E-mail: neetugju@yahoo.co.in

**Received: 01 January 2016, Revised: 29 February 2016 and Accepted: 19 May 2016**

DOI: 10.5185/amlett.2017.6398
www.vbripress.com/aml

## Abstract

In the present work, the results of microstructure, dielectric and ferroelectric investigation of microwave sintered $CaCu_3Ti_4O_{12}$ (CCTO) ceramic with different heating rate are presented. Scanning electron micrographs revealed that grain size decreases from 1.167 µm to 0.744 µm with increased heating rate from 10ºC/min. to 50ºC/min which can be explained on the basis of phenomenological kinetic equation for grain growth. Dielectric response also found to influence by heating rate. The CCTO ceramic sintered with 50ºC/min. exhibited highest dielectric constant ($\varepsilon_r$~3915) with nominal losses (0.10) at room temperature in broad frequency range from $10^2$Hz-$10^5$Hz. Cole-Cole plots revealed the change in grain boundary resistivity mainly caused by the oxygen vacancy activities and affected by varying sintering heating rate. An anomaly observed for 50ºC/min heating rate due to trapping of oxygen at grain boundaries. The remnant polarization and coercive field for CCTO ceramic sintered with 50ºC/min were 0.1 µC /cm$^2$ and 1.477 kV /cm respectively. Remnant polarization found to decrease while the coercive field increases with increasing heating rate applying these are micro-structural dependent. Copyright © 2017 VBRI Press.

**Keywords:** $CaCu_3Ti_4O_{12}$, dielectric, ferroelectric, P-E loop, microwave, heating rate.

## Introduction

Perovskite structured ceramics are well notorious due to their giant dielectric constant ($\varepsilon_r$) which makes these materials technically important for microelectronic application such as capacitors and capacitive mechanisms based memory, especially static and dynamic random access memories etc. [**1, 2**]. Both relaxor and ferroelectric materials undergo a phase transition in dielectric constant as a function of temperature resulting in higher volatility of the devices with temperature variation. On the contrary $CaCu_3Ti_4O_{12}$ (CCTO) ceramic having bcc perovskite type structure with Im3 space group has captivated large attention because of its room temperature giant dielectric constant ($\mathcal{E}_r$~$10^5$) over a wide range frequency ($10^2$Hz-$10^6$Hz). Also, dielectric constant is temperature independent in 100-600K range and without any changes in phase or long range crystal structure as well [**3-5**]. Till the date many hypotheses have been put forward to enlighten the giant dielectric response in CCTO ceramics, but its origin still controversial. Various models have been proposed for intrinsic effect to understand the giant dielectric response viz. mixed-valent structure [**6**], nanoscale disorder [**7**] and Polaron relaxation model [**8**]. For the extrinsic effect, the internal barrier layer capacitor (IBLC) model is widely believed origin for giant dielectric response and at the present IBLC model of extrinsic mechanism is most acceptable [9]. Subramanian and Sinclair *et al* reported that the giant dielectric response in CCTO due to internal barrier layer capacitance (IBLC) effect, resulting from capacitances at twin boundaries and grain boundaries capacitances in single and polycrystalline CCTO respectively [**4, 10**]. According to Lunkenheimer *et al*, huge dielectric response is due to interfacial polarization effect between sample surface and electrodes [**11**]. J. Yang *et al* reported the existence of both grain boundaries and electrode effect in CCTO ceramic contributing to high dielectric constant [**12**]. Recently CCTO ceramics reported to exhibit ferroelectric-like hysteresis loop despite of having space group Im3, remnant polarization and coercive field were found to processing condition and micro-structural dependent [**13, 14**]. Moreover, the dielectric properties of CCTO are highly dependent on processing parameters such as sintering time, temperature and cooling atmosphere etc. [**10, 15**]. Usually, sintering of CCTO ceramic is carried out by conventional furnace using resistive heating, which requires high sintering temperature and long duration. Also, some major problems encountered by conventional sintering are low density, nonuniform microstructure and sometimes sample cracking due to heat delivered from surface to bulk by thermal conduction. Microwave sintering of materials is finding widespread applications due to its reduced processing time, temperature and energy cost with decreased grain size, enhanced microstructure and others properties of ceramics which are currently unattainable by conventional sintering [**16, 17**]. But the effect of various microwave parameters such as sintering temperature, sintering time and heating rate, are still a topic of research for controlled microstructural development. Heating rate found to affect microstructure evolution and densification, so act as important parameter in microstructural control. However, till now, much work has been reported which reflects the effect of processing condition on structural and dielectric properties using conventional heating. But in recent years due to technological development and need for quick and efficient synthesis of ceramics use of microwave increased dramatically due to many advantages as discussed formerly. As in case of microwave heating except the soaking time, one more parameter which intensely affects the microstructure of ceramics is heating rate. So it becomes necessary to alleviate the heating rate to control microstructural evolution in ceramics. In the present work efforts were made to correlate the microwave heating rate with structural and electrical properties of $CaCu_3Ti_4O_{12}$ ceramic. The CCTO ceramics have been fabricated by solid-state reaction route and sintered using microwave furnace with different heating rates. The effect of the microwave heating rate on microstructural, dielectric and ferroelectric properties of CCTO has been investigated.

## Experimental

### *Materials/ chemicals details*

The $CaCu_3Ti_4O_{12}$ ceramics investigated in this work, were fabricated using high purity $CaCO_3$ (99%, Sigma Aldrich), CuO (99%, sigma Aldrich) and $TiO_2$ (99%, Sigma Aldrich) St. Louise, U.S.A, as the starting materials.

### *Material synthesis*

Stoichiometric ratios of the starting materials were ball milled for 10 hours using zirconium balls in distilled water at 500 ball's RPM. DTA and TG analysis carried out to determine adequate reaction temperature and decomposition of ball milled CCTO powder. These measurements were performed using a Q-600 SDT-TA instrument from room temperature to 1250K with a heating rate of 5ºC/min, in air. Then prepared $CaCu_3Ti4O_{12}$ powder was calcined at 1273K for 10 hours in the air using a conventional furnace and single phase formation of thus prepared samples were confirmed by X-ray diffraction technique. The calcined powder was ground thoroughly well, then mixed with 3 wt. % aqua's solution of polyvinyl alcohol (PVA) and pressed into disks of diameter ~ 10 mm and thickness ~ 1.2 mm under pressure of 12 MP for 5 minutes. The disks were sintered for 60 minutes at 1353K with different heating rate 10, 30 and 50°C/min. using microwave furnace, then cool down to room temperature in closed furnace. These prepared samples were abbreviated as CCTO-10, CCTO-30 and CCTO-50 respectively.

### *Characterizations*

The single-phase formation of microwave sintered samples were examined by X-ray diffraction on a diffraction-meter (XRD; MiniFlex2 Rigaku Japan) with Cu $K_\alpha$ radiation in a wide range of 2θ ($20° \leq 2\theta \geq 80°$) at a scanning rate 2 degree/minute, operated at 30 kV and 15 mA. The microstructure of fractured pellets was investigated using scanning electron microscope. The dielectric properties as a function of temperature (300-430K) in the frequency range (0.1Hz-10MHz) were analyzed by an impedance /gain-phase analyzer (Alpha-A high frequency analyzer, Nova-control Tech.). Polarization vs. electric field (P-E) hysteresis loops were sketched at room temperature using automatic P-E loop tracer (Marine India) with samples immersed in silicone oil to prevent electrical breakdown.

## Results and discussion

### *Thermal analysis and phase composition*

**Fig. 1** shows the DTA-TG analysis of the dried CCTO powder with heating rate 5°C /min from room temperature to 1250K. The TG curve indicates total weight loss about 11.6 % up to 1250K related to decomposition and organic matrix combustion process.

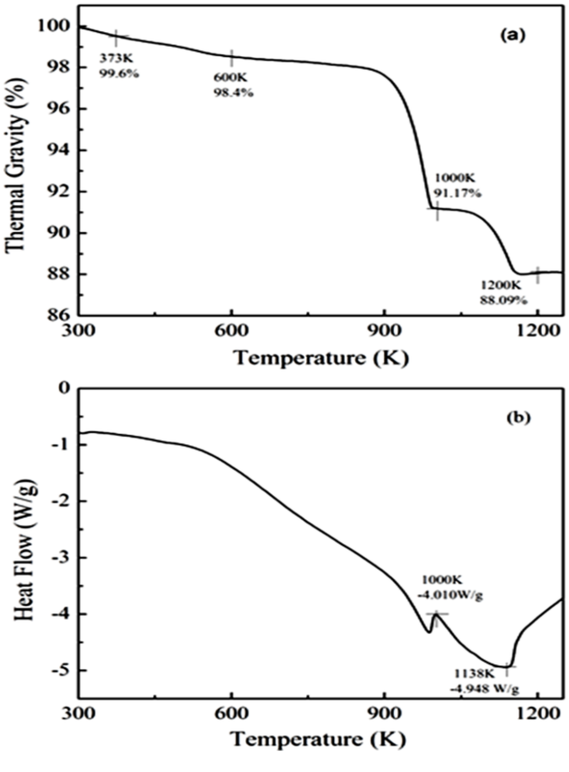

**Fig. 1.** DSC/TGA curve for dry $CaCu_3Ti_4O_{12}$ sample powder.

The TG curve shows the process of weight loss in three stages with increasing temperature up to 1250K. The first stage of TG curve start from 373K to 600K related to physically absorbed water loss (1.2%). The second one from 900K to 1000K which shows major weight loss (7.3%) may be due decomposition of $CaCO_3$ to release $CO_2$ and burnout of organic matrix to form intermediate complex supported by an exothermic peak in DTA curve at 999K. The third one with very low (3.1%) weight loss from 1000K to 1200K with an endothermic peak in DTA at 1138K, accompanied by $TiO_2$ addition with intermediate complex to form final product CCTO. DTA curve shows only one exothermic peak at 999K in temperature range (900-1000K) indicating that no phase transformation occurs in precursor below 999K [18-20]. After that no further weight loss was noticed up to 1250K. Which indicate the formation of CCTO phase around 1200K, hence to ensure the synthesis efficiency and single phase formation calcinations temperature was fixed at 1273 K.

**Fig. 2** illustrates the X-ray diffraction patterns of all microwave sintered CCTO ceramic samples at 1353K with different heating rate.

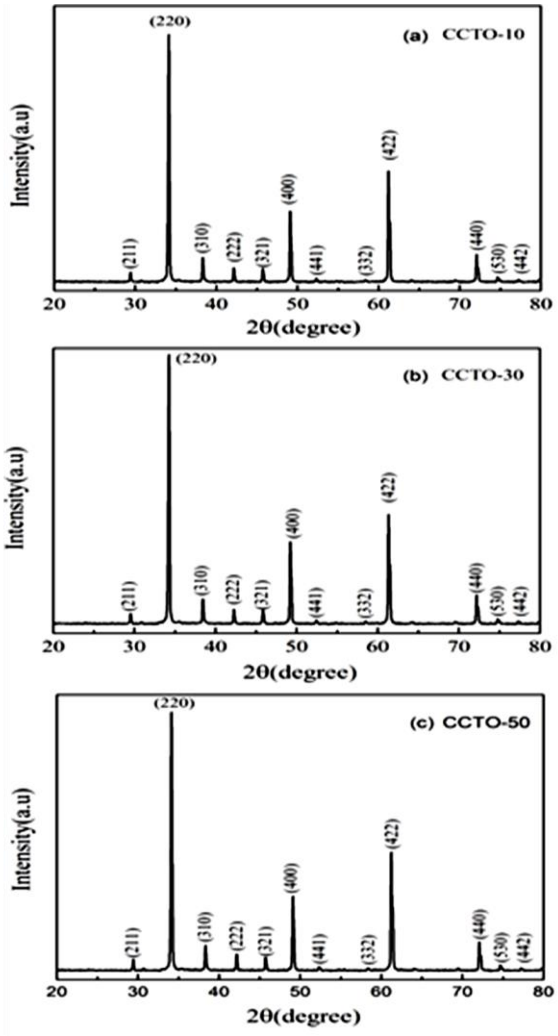

**Fig. 2.** X-ray diffraction patterns of $CaCu_3Ti_4O_{12}$ ceramics sintered with heating rate (a) 10ºC/min (b) 30ºC/min and (c) 50ºC/min.

All prepared samples show similar diffraction profiles and diffraction peaks. The crystal structure of these samples was identified as the cubic pervoskite phase and all peaks were indexed with JCPDS Card No.: 751149. The lattice constant of CCTO samples were calculated using Bragg's law for high intensity diffraction peaks. Theoretical X-ray density of prepared CCTO samples were calculated from the value of lattice constant by equation

$$D_x = \frac{2M}{Na^3} g/_{cm^3} \qquad (i)$$

where, M is molecular weight, N is the Avogadro number, and 'a' is lattice constant. While the bulk densities were calculated by the Archimedes principle using xylene. With the help of theoretical density ($D_x$) and bulk density ($D_{bulk}$), the porosity was calculated using equation

$$Porosity\ (\%) = \left(1 - \frac{D_{bulk}}{D_x}\right) \times 100 \qquad (ii)$$

**Table. 1.** Summary of structural data of lattice constant, X-ray density, bulk density, porosity and grain size.

| Sample | Lattice constant a (Å) | X-ray density $D_x$ (g/cm$^3$) | Bulk density $D_b$ (g/cm$^3$) | Porosi-ty (P) (%) | Grain size (μm) |
|---|---|---|---|---|---|
| CCTO-10 | 7.426 | 4.980 | 4.599 | 7.6 | 1.167 |
| CCTO-30 | 7.392 | 5.049 | 4.799 | 4.9 | 0.842 |
| CCTO-50 | 7.446 | 4.940 | 4.751 | 3.8 | 0.744 |

The values of all these structural parameters are summarized in Table 1. It could be seen from the calculated data that increasing heating rate decreases the lattice constant from 7.426 Å to 7.392 Å may be attributed to compression of unit cell, and then again increase at heating rate 50°C/min up to 7.446 Å. While the bulk density found to be increasing continuously with heating rate due to the grain coarsening and thereby decreasing porosity. The maximum relative density observed at 50°C/min which is 96.17% of X-ray density corresponding to bulk density is 4.751 g/cm$^3$, with lowest porosity 3.8%. This small variation in porosity and density sufficient to causes the adequate difference in dielectric behavior.

### *Microstructure*

Surface morphology of the microwave sintered $CaCuTi_4O_{12}$ ceramics were investigated using SEM micrographs of fractured surface, as shown in **Fig. 3** (a-c) of CCTO-10, CCTO-30 and CCTO-50 respectively. It is obvious from the SEM images that average grain size decreases with increasing heating rate which can be explained on the basis of phenomenological kinetic equation for grain growth for constant heating rate [**16**].

$$G_0^n + \frac{k_0}{\alpha}\int_{T_0}^{T}\exp\left(-\frac{\mathrm{Q}}{\mathrm{KT}}\right)\,\mathrm{dT} \qquad \text{(iii)}$$

where, G and $G_0$ are the grain sizes at holding time t and t=0 respectively, while n and $k_0$ are constant for particular grain growth mechanism. Q is activation energy for grain growth; k is the Boltzmann constant, α is heating rate

$$T = T_0 + \alpha t \qquad \text{(iv)}$$

where, t represents heating cycle time. The experimental calculated values of grain size are in well agreement with equation (3) and grain size is inversely proportional to heating rate α (**Table 1**). It was observed from Table.1 that the average grain size decreases with increasing heating rate. The CCTO sample sintered at 1353K with heating rate 50°C/min, show smallest grain size (0.744 µm). Also the porosity of all ceramic samples was found to significantly affect by the heating rate. Lowest porosity (3.8%) was obtained in microwave sintered sample CCTO-50 with heating rate 50°C/min. This difference in grain size may be due to the difference in relative contribution of grain, grain boundary and lattice diffusion with different heating rate [**16**].

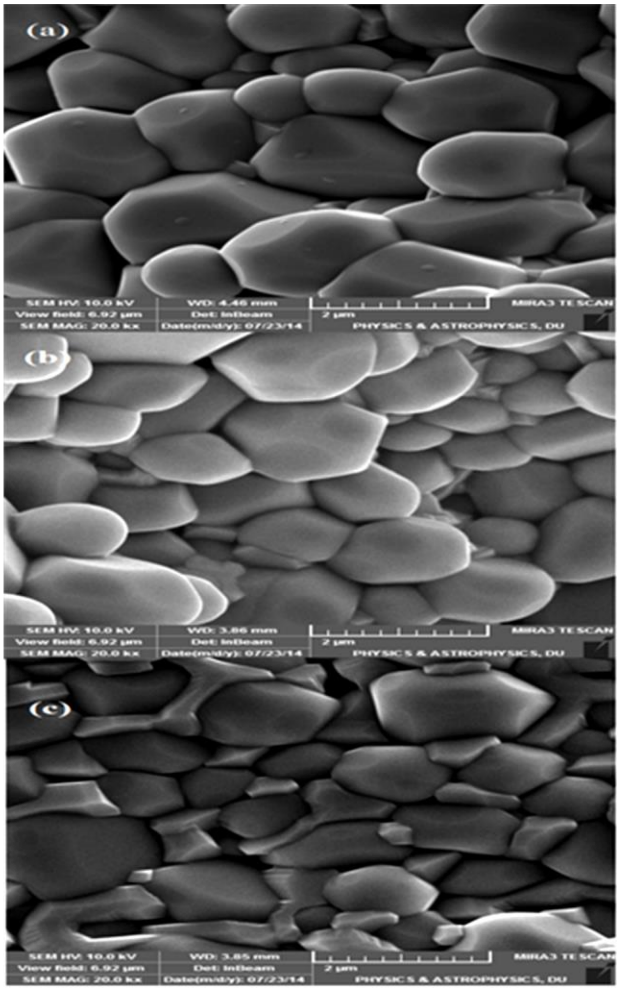

**Fig. 3.** SEM micrograph of $CaCu_3Ti4O_{12}$ ceramics sintered with heating rate (a) 10ºC/min (b) 30ºC/min and (c) 50ºC/min.

*Dielectric analysis*

The dielectric properties originate the way for potential applications of ceramics in microelectronic devices. **Fig. 4** (a-c) shows the frequency dependence of dielectric constant for all prepared CCTO ceramics. **Fig. 4** depicts that dielectric constant remains nearly frequency independent at higher frequencies and shows dispersion at lower frequencies as temperature increases from room temperature to 423K in all CCTO ceramic samples.

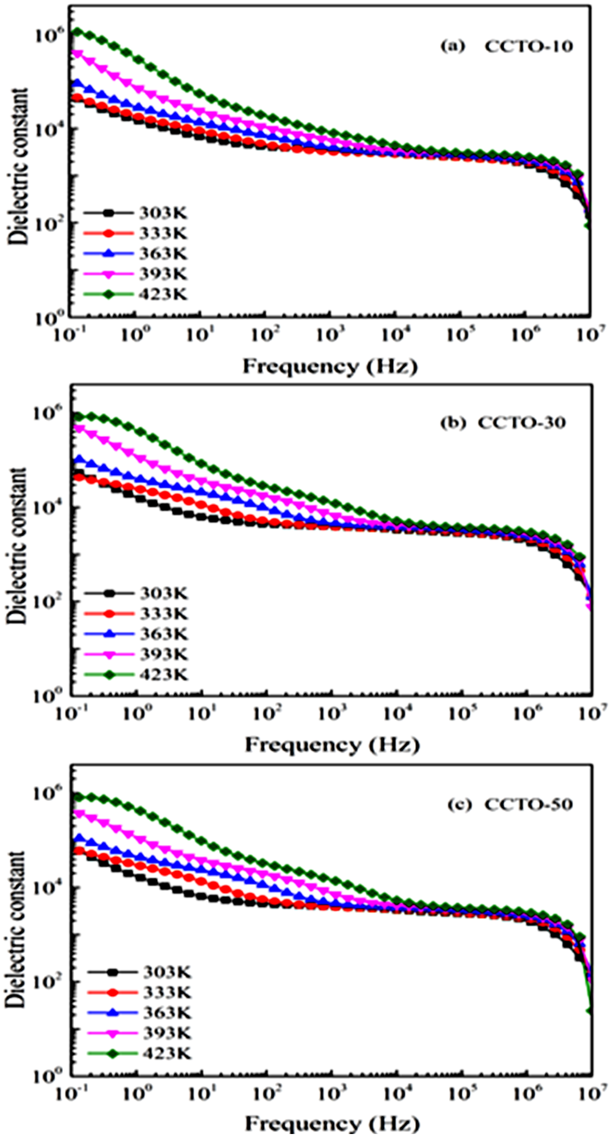

**Fig. 4.** Frequency dependence of dielectric constant ($\varepsilon_r$) at different temperature for $CaCu_3Ti_4O_{12}$ ceramics sintered with heating rate (a) 10ºC/min (b) 30ºC/min and (c) 50ºC/min.

This dispersion may be attributed to interfacial polarization caused by blockage of charge carriers at electrode interface due to low frequency applied electric field. Also at higher frequency ionic dipoles unable to follow the field reversal which decrease the dielectric constant [**19, 21**]. The perusal of dielectric data reveals that dielectric properties are thermally activated in low frequency region and becomes thermally stable when the frequency of applied field increased above 10 kHz. The low frequency dielectric relaxation below 1 kHz was appeared in dielectric spectra of CCTO-30 and CCTO-50 at temperatures except room temperature and corresponding dielectric relaxation peak ($f_p$) shifts towards higher frequency with increasing temperature. This behavior is in well agreement with the previously reported data by J.L. et al. Another relaxation around 1 MHz was observed for all prepared CCTO ceramics over the whole studied temperature range and associated with IBLC effect of semi conductive grains and insulating grain boundaries [**22**].

Usually, $CaCu_3Ti4O_{12}$ ceramics have high dielectric constant for large grain size as dielectric properties of ceramics are closely related to its microstructure. However, sample sintered with 50°C/min has highest dielectric constant despite of having small grain size may be attributed to increased oxygen vacancies and density with enhanced homogeneity at higher heating rate [**1, 19**]. Hence formed free electrons in CCTO samples according to equation (v),

$$O_0(Oxygen) \rightarrow V_0^{2+}(Oxygen\ vacancy) + 2e^- + \frac{1}{2}O_2 \quad \text{(v)}$$

Which causes space charge distribution on grain boundary and thus produced space charge polarization contributes to high dielectric constant [**23, 24**].

**Fig. 5** (a-c) shows the variation of dielectric loss factor (tanδ) as a function of frequency and temperature for all prepared CCTO ceramics sintered with different heating rate. Dielectric losses are strongly temperature dependent in low frequency range while remains almost constant at higher frequencies. Dielectric relaxation behavior observed in low frequency range in all prepared CCTO ceramics samples can be explained on the basis of space charge polarization arises due to contact of two different phases of grain-grain boundaries with different electrical conductivity [25, 26]. The curve demonstrates a plateau with lowest dielectric losses over frequency range from 100 Hz to 0.1MHz for all studied samples. Three different types of temperature dependence were observed over this frequency range. In low frequency region, the dispersion in dielectric loss with temperature is more pronounced while the trend is reversed in high frequency region. Further a plateau with lowest value observed in middle frequency region tends to diminished as temperature rises from room temperature to 423K. The same results also reported earlier for CCTO ceramics [**1, 27**]. The zoom view of this curve over frequency range 100 Hz to 1MHz for CCTO-50 is shown as inset in Fig.5(c). This behavior can be explaining with the knowledge of two types of dielectric loss mechanism in dielectric materials, namely, ‘resistive loss mechanism and relaxation loss of dipole [**28, 29**]. The energy consumed by free charge carriers causes resistive losses while expenditure of energy during the relaxation of dipole defines relaxation loss mechanism [**30**]. The expression for dielectric loss is given by with certain conditions as $R_{gb}>>R_g$, $C_{gb}\sim C_p>>C_g$ and $\omega R_g C_{gb}<<1$

$$\tan\delta = \frac{1}{\omega R_{gb}\ C_p} + \omega R_g\ C_p \quad \text{(vi)}$$

The low frequency dispersion can be well explained using first term of the above equation and in high frequency region second term becomes more predominant, where tanδ increases linearly with frequency when f > $10^5$ Hz. The variation shown by the experimental data is well in agreement with above equation for all prepared CCTO ceramics.

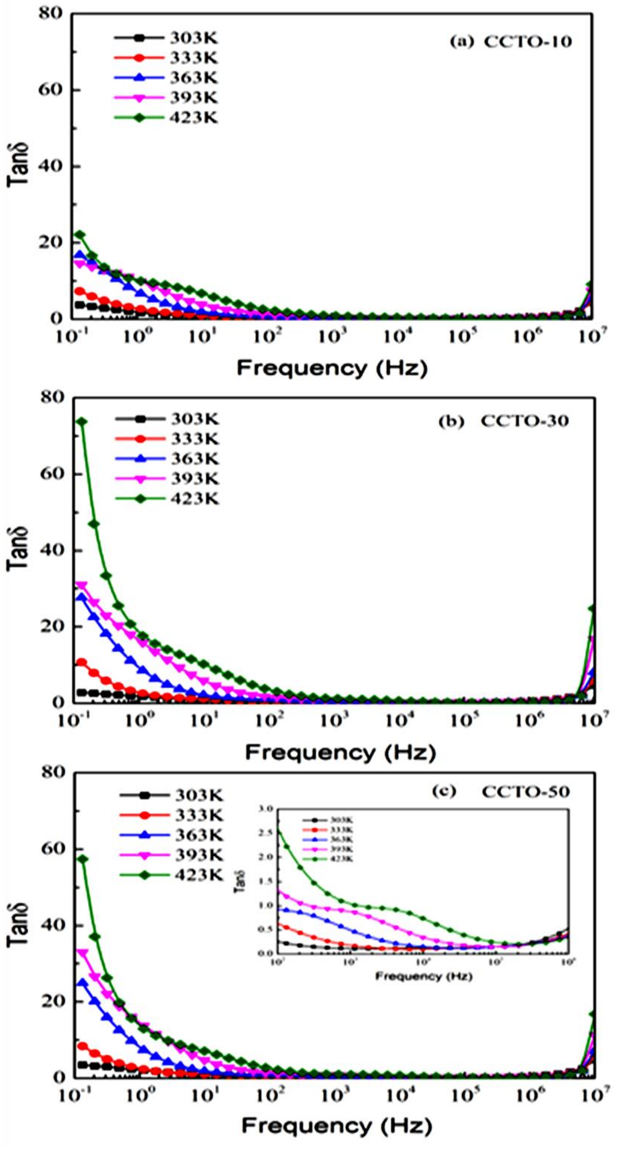

**Fig. 5.** Frequency dependence of dielectric loss (tanδ) of $CaCu_3Ti4O_{12}$ ceramics at different temperature for $CaCu_3Ti4O_{12}$ ceramics sintered with heating rate (a) 10ºC/min (b) 30ºC/min and (c) 50ºC/min. Inset: Zoom view of tanδ isotherms over frequency range $10^2$ Hz to $10^6$ Hz.

**Fig. 6** (a-b) depicts the comparative dielectric behavior of all the prepared CCTO ceramics over wide frequency range at room temperature. Fig.6 (a) compares the dielectric loss curve for CCTO samples sintered at different heating rate. Lowered dielectric loss factor was observed when heating rate increased from 10ºC/min to 50ºC/min in low frequency region (below 1kHz) while the trends is reversed in high frequency region (above 100kHz). The comparative lower resistivity value of grain boundaries for CCTO-30 and CCTO-50 (see **Table 2**) and relatively more grain coarsening at higher heating rate [**31**] results in low resistive loss contribution at low frequencies of applied field. The perusal of dielectric data indicates occurrence of the dielectric dispersion below 100 Hz and other one above 1 MHz with almost same value of dielectric constant irrespective of sintering heating rate as shown in **Fig. 6** (b). In frequency window above 100 Hz and below 1 MHz the curves show a plateau region and dielectric constant value enhanced significantly for higher heating rate. The zoom view of this region is also shown as inset of **Fig. 6** (b). This increase in dielectric constant may be attributed to enhanced densification at higher heating rate. It is clear from **Fig. 6** (a & b) that stable and enhanced dielectric constant with lowered dielectric loss in low radio frequency range ($10^3$ Hz to $10^5$ Hz) can be achieved with fast heating rate which makes them suitable materials for microelectronics.

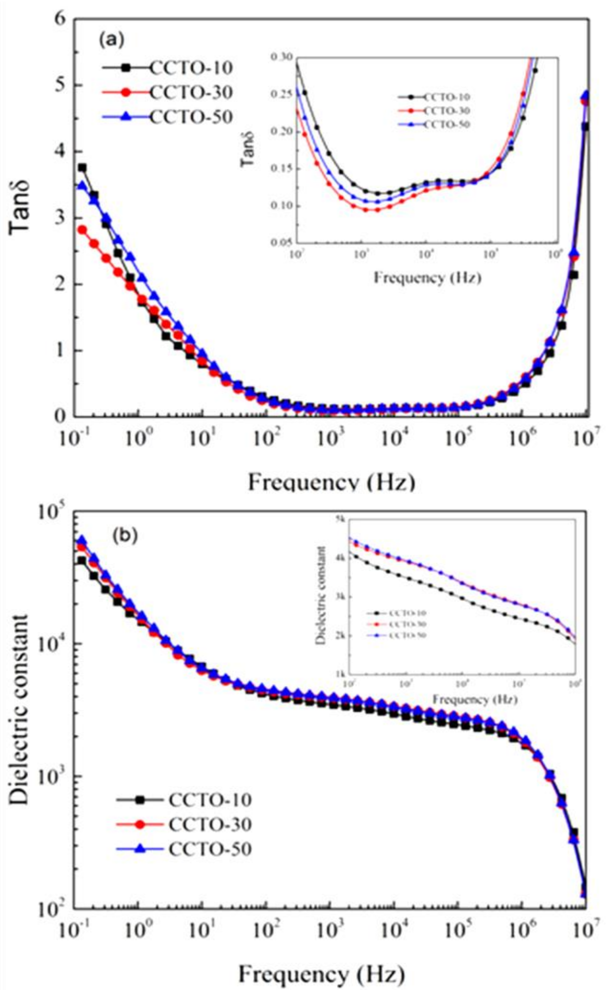

**Fig. 6.** Frequency dependence of (a) dielectric loss (tanδ) and (b) dielectric constant ($\varepsilon_r$) at room temperature for CCTO-10, CCTO-30 and CCTO-50. Inset: Zoom view over frequency range $10^2$ Hz to $10^6$ Hz.

**Fig. 7** (a-b) shows the temperature dependence of dielectric constant ($\varepsilon_r$) and dielectric loss (tanδ) at 1 kHz for all ceramic samples sintered with different heating rate. The result evidences the existence of thermally stable dielectric loss and dielectric constant over temperature range 300 to 423K for all studied samples. The highest dielectric constant was observed for CCTO-50 among all prepared samples. The values of dielectric losses (observed for CCT0-10, CCTO-30 and CCTO-50 ceramics are 0.12, 0.09 and 0.10 respectively at room temperature.

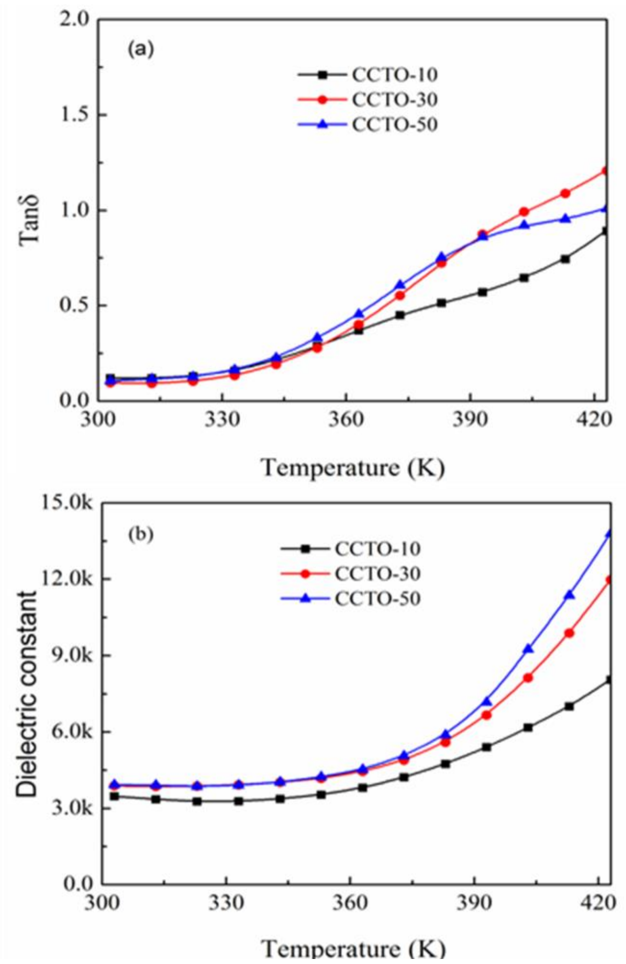

**Fig. 7.** Temperature dependence of (a) dielectric loss (tanδ) and (b) dielectric constant ($\varepsilon_r$) for CCTO-10, CCTO-30 and CCTO-50 ceramics at 1 kHz.

### *Conductivity*

**Fig. 8** shows the frequency dependence of ac conductivity at 423 K for all CCTO samples sintered with different heating rate. The observed conductivity spectra exhibit two plateau regions separated by dispersive conductivity. This separation appears clearer in CCTO-30 and CCTO-50 samples and may attributes to comparative smaller grain size of these samples. This behavior of conductivity spectra can be explained by Jonschar double power law [**32**].

$$\sigma(\omega) = \sigma_{dc} + A\omega^{n1} + B\omega^{n2} \qquad \text{(vii)}$$

where A, B, $n_1$ and $n_2$ are fitting parameters and are temperature dependent constant. DC conductivity is represented by $\sigma_{dc}$ term in above equation. The existence of two slopes reveals the contribution of two relaxation process in bulk conductivity of these materials. Low frequency dispersion occurs due to long time relaxation processes in grain boundaries with large capacitance values while second dispersion in high frequency region corresponds to short time relaxation of charge carriers within grains having low capacitance values.

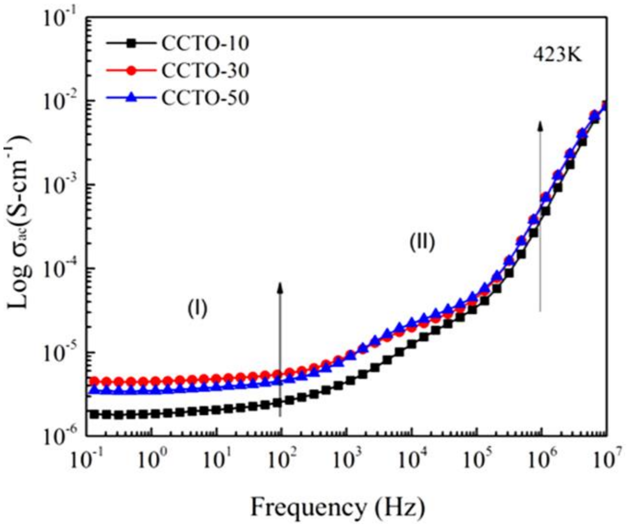

**Fig. 8.** Frequency dependences of ac conductivity at 423K for CCTO-10, CCTO-30 and CCTO-50 ceramics.

The existence of two relaxation processes also supported by analysis of dielectric relaxation peaks in low and high frequency region of these studied samples. The samples CCTO-30 and CCTO-50 have nearly same value of conductivity and exhibit same behavior. The ac conductivity of all prepared samples, increase slowly with increasing frequency in low frequency range, while increases rapidly at higher frequencies which can be explain on the basis of interfacial effect [**19**]. It is observed from the **Fig. (9)** that with increasing heating rate, the ac conductivity increased in region (II) as conductivity in this region mainly due to grains and the possibilities of creations of more oxygen vacancies in grains with increase in heating rate causes enhanced conductivity. Whereas an anomaly is observing in the conductivity of region (I), where conductivity of CCTO-50 is less than that of CCTO-30. In this region (low frequencies region) the contribution to conductivity is mainly due to grain boundaries. So, there may be possibility of trapping of excess oxygen from grains at grain boundaries which may result increased resistivity of CCTO-50. Hence variation in conductivity with heating rate mainly due to oxygen vacancies and thus produced space charge in grain boundaries [**33**]. The analysis of conductivity spectra reveals the occurrence of high conducting grains and more resistive grain boundaries with fast heating rate. The same is desired for improved dielectric properties of CCTO ceramics according to IBLC model [**22**].

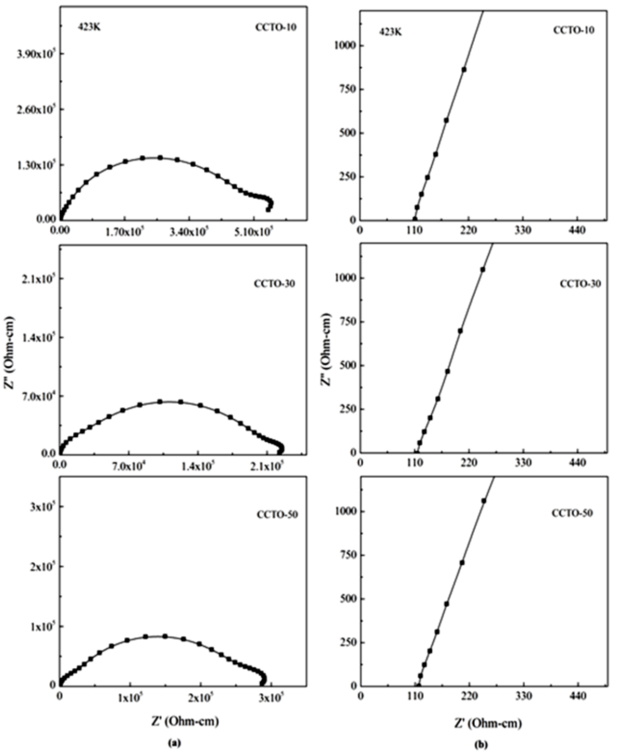

**Fig. 9.** (a) Complex impedance plots at 423 K for CCTO-10, CCTO-30 and CCTO-50 ceramics (b) Expanded view of impedance plots in high frequency region.

### *Impedance analysis*

Impedance spectroscopy is powerful technique used to correlate the microstructure of materials to its electrical behavior and distinguish the contribution of grain and grain boundary. Impedance plots (Z' and Z") for CCTO-10, CCTO-30 and CCTO-50 ceramics at 423K are shown in Fig.9 (a) while Fig.9 (b) demonstrates high frequency expanded view of impedance. These plots of impedance can predict the variation of grain and grain boundary ($R_{g,}$, $R_{gb}$) resistivity as well as conducting behavior. Non zero intercepts of impedance semicircle on Z' axis in high frequency region corresponds to grain resistance ($R_g$) while intercept in lower frequency region corresponds to grain boundary resistance ($R_{gb}$) [19]. The grain and grain boundary contribution to total resistance were calculated from nonzero intercepts on Z' axis of impedance plots and are given in **Table 2**.

**Table 2.** Summary of dielectric constant ($\varepsilon_r$), dielectric loss (Tanδ) at room temperature, grain resistance ($R_g$) and grain boundary resistance ($R_{gb}$) at 423K of all microwave prepared samples.

| Sample | $\varepsilon_r$ at 1kHz | Tanδ at 1kHz | $R_g$(Ω-cm) | $R_{gb}$(Ω-cm) |
|---|---|---|---|---|
| CCTO-10 | 3470.6 | 0.12 | 111 | $5.1x10^5$ |
| CCTO-30 | 3883.3 | 0.09 | 115 | $2.1x10^5$ |
| CCTO-50 | 3915.8 | 0.10 | 117 | $2.7x10^5$ |

Reduction in semicircular arc radius with increasing heating rate depicts the grain boundary resistivity ($R_{gb}$)

decreased from 5.1x$10^5$ Ω-cm to 2.1x$10^5$ Ω-cm for samples CCTO-10 and CCTO-30 respectively. Whereas an anomaly is shown by CCTO-50 where grain boundary resistivity increases slightly up to 2.7x $10^5$ Ω-cm may be attributed to trapping of excess oxygen at grain boundaries of CCTO-50 as discussed in previous section.

### *P-E analysis*

Figure 10 (a-c) shows P.E hysteresis loop traced at 50 Hz, room temperature for all CCTO ceramics samples sintered with different heating rate. The values of remnant polarization ($P_r$), coercive field ($E_c$) and maximum polarization ($P_{max}$) are summarized in **Fig. 10**.

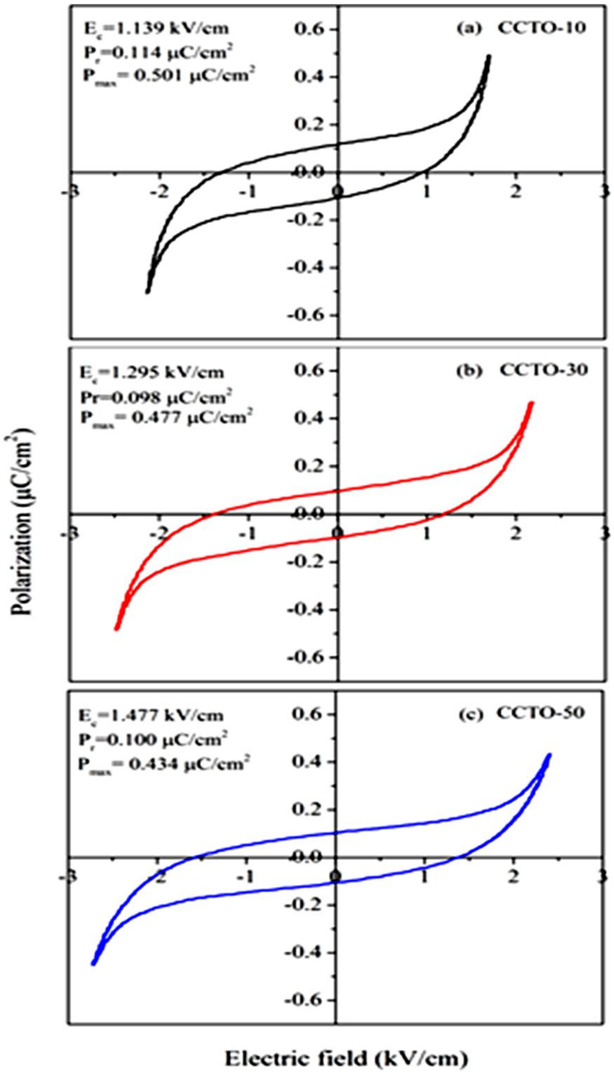

**Fig. 10.** Room temperature P-E hysteresis loops for CCTO-10, CCTO-30 and CCTO-50 ceramics.

It can be observed from Fig. that the value of remnant polarization and maximum polarization decreases with increasing heating rate. As the grain size decreases, the number of grain boundaries increases which increase the space charges polarization on grains boundaries. As a result, the polarization on grain surface is excluded and thus formed depletion layer depolarized the field reducing the net polarization with smaller grain size [**34**]. As obvious from microstructural studies that average grain size decreases with increasing heating rate causing remnant polarization decreases as grain size get smaller. Our results are in good agreement with results reported by C.A. Randall *et al*. [**35**]. Increase in $E_c$ with increasing heating rate may be due to decrease in average grain size [**35, 36**]. When average grain size decreases result in increasing total numbers of grain boundaries which may uplift the Schottky barriers formed at grains and grain boundaries [**10, 37, 38**] cause to increasing in the value $E_c$. Hence difference in values of $E_c$ can be understood by the difference produced in grain size due to difference in heating rate during sintering.

## Conclusion

In the current research work, the effect of microwave heating rate has been demonstrated on sintering of $CaCu_3Ti_4O_{12}$ ceramic. It was found that higher heating rate (50ºC/min) can fabricate more uniform and dense microstructure. The highest relative density was achieved for 50°C/min, which is 96.17% of X-ray density, with lowest porosity 3.8%. Analysis of SEM images evidences that grain size is significantly affected by heating rate and decreased from 1.167 µm to 0.744 µm with increasing heating rate from 10ºC/min. to 50ºC/min. The improved dielectric properties ($\varepsilon_r$~3915) with nominal dielectric losses (tanδ~ 0.10) in broad frequency range from $10^2$ Hz to $10^5$ Hz were attained for $CaCu_3Ti_4O_{12}$ ceramic sample CCTO-50. Conductivity found to increase with increasing heating rate from 10ºC/min. to 30ºC/min but an anomaly was observed in CCTO-50 ceramic in low frequency region attributed to trapping of excess oxygen from grains at grain boundaries. It was evident from P.E loops that remnant polarization ($P_r$) and maximum polarization ($P_{max}$) decreases while the coercive field increased with increasing heating rate applying these depend on microstructure. The heating rate (50ºC/min) was found most appropriate to alleviate structural and electrical properties synthesized ceramics.

### Acknowledgements

The authors are thankful to UGC (41-853 (2012)) for providing financial support and fellowship. Authors are also thankful to DST, New Delhi (FIST Scheme), AICTE (8023/RID/RPS), and DU New Delhi for providing XRD, P.E Loop Tracer, and Impedance analyzer/SEM facilities respectively

### References

1. H. Wang, S. Li, J. He, and C. Lin, *J. Mater Sci.: Mater Electron*. **2014,** 25, 1842. **DOI:** 10.1007/s10854-014-1807-4
2. C. Kai, L. Wei, L. Yun-Fei, B. Peng, L. Xiao-Mei, and Z. Jin-Song, *Chin.Phys.Lett.* **2004,** 21, 1815. **DOI:** 10.1088/0256-307X/21/9/039
3. A.P. Ramirez, M.A. Subramanian, M. Gardel, G. Blumberg, D. Li, T. Vogt, and S.M. Shapiro, *Solid State Commun.* **2000,** 115, 217. **DOI:** 10.1016/S0038-1098(00)00182-4
4. M.A. Subramanian, D. Li, N. Duan, B.A. Reisner, and A.W. Sleight, *J. Solid State Chem.* **2000,** 151, 323. **DOI:** 10.1006/jssc.2000.8703

5. M.A. Subramanian, and A.W. Sleight, *Solid State Sci.* **2002,** 4, 347. **DOI:** 10.1016/S1293-2558(01)01262-6
6. Y. Wang, L. Ni, and X.M. Chen, *J. Mater. Sci.: Mater. Electron.* **2011,** 22, 345. **DOI:** 10.1007/s10854-010-0140-9
7. Y. Zhu, J. C. Zheng, L. Wu, A. I. Frenkel, J. Hanson, P. Northrup, and W. Ku, *Phys. Rev. Lett.* **2007,** 99, 037602. **DOI:** 10.1103/PhysRevLett.99.037602
8. C. C. Wang, and L. W. Zhang, *Appl. Phys. Lett.* **2007,** 90, 142905. **DOI:** 10.1063/1.2719608
9. L. Zhang, and Z. J. Tang, *Phys. Rev. B.* **2004,** 70, 174306. **DOI:** 10.1103/PhysRevB.70.174306
10. D. C. Sinclair, T. B. Adams, F. D. Morrison, and A.R. West, *Appl. Phys. Lett.* **2002,** 80, 2153. **DOI:** 10.1063/1.1463211
11. P. Lunkenheimer, R. Fichtl, S. G. Ebbinghaus, and A. Loidle, Phys. *Rev. B*, **2004,** 70, 172102. **DOI:** 10.1103/PhysRevB.70.172102
12. J. Yang, M.R. Shen, L. Fang, *Mater. Lett.* **2005,** 59, 3990. **DOI:** 10.1016/j.matlet.2005.07.049
13. B. Shri Parkash and K. B. R. Verma, *Appl. Phys. Lett*. **2007,** 90, 082903. **DOI:** 10.1063/1.2539724
14. R. Kashyap, T. Dhawan, P. Gautam, O.P. Thakur, N.C. Mehra, and R.P. Tandon, *Modern Physics Letter B*, **2010,** 24, 1267. **DOI:** 10.1142/S021798491002327X
15. B. A. Bender, and M. J. Pan, *Mater. Sci. Eng. B*. **2005,** 117, 339. **DOI:** 10.1016/j.mseb.2004.11.019
16. G. F. Xu, I. K. Lloyd, Y. Carmel, T. Olorunyolemi, and O. C. Wilson, *J. Mater. Res.* **2001,** 16, 2850. **DOI:** 10.1557/JMR.2001.0393
17. J.D Katz, *Annual Review of material Science*, **1992,** 22, 153. **DOI:** 10.1146/annurev.ms.22.080192.001101
18. X. Ouyang, S. Huang, W. Zhang, P. Cao, Z. Huang, and W. Gao, *J. Solid. State. Chem.* **2014,** 211, 58. **DOI:** 10.1016/j.jssc.2013.12.009
19. L. Singh, U. S. Rai, A. K. Rai, and K. D. Mandal, *Electronic Materials Letters.* **2013,** 9, 107. **DOI:** 10.1007/s13391-012-2095-x
20. S. Sharma, S. S. Yadav, M. M. Singh, and K.D. Mandal, *J. Advance Dielectrics.* **2014,** 4, 1450030. **DOI:** 10.1142/S2010135X14500301
21. W. Q. Ni, X. H. Zheng, and J. C. Yu, *J. Mater. Sci.* **2007,** 42, 1037. **DOI:** 10.1007/s10853-006-1431-7
22. J. L. Zhang, P. Zheng, S. F. Shao, W. B. Su and C. L. Wang, *Ferroelectric.* **2007,** 356, 85. **DOI:** 10.1080/00150190701509264
23. R. Venkataraman, P. R. Richard, and P.D. Vinayak, *J. American Ceramic Society*. **1997,** 80, 1131. **DOI:** 10.1111/j.1151-2916.1997.tb02955.x
24. V. Hangloo, R. Tickoo, K. K. Bamzai, and P. N. Kotru, *J. materials chemistry and physics*. **2003,** 81, 152. **DOI:** 10.1016/S0254-0584(03)00181-0
25. E. A. Patterson, S. Kwon, C. C. Huang, and D. P. Cann, *Appl. Phys. Lett.* **2005,** 87, 182911. **DOI:** 10.1063/1.2126142
26. L. Wang, Q. Shenyu, C. Nan, and D. Guoping, *J. Mater. Sci. Tehnol.* **2010,** 26, 682. **DOI:** 10.1016/S1005-0302(10)60107-7
27. B. Wang, Y. Ping Pu, H-Dong Wu, K Chen and N. Xu, *Ceram. International*. **2013,** 39, S525. **DOI:** 10.1016/j.ceramint.2012.10.127
28. L. Feng, X. Tang. Y. Yan, X. Chen, Z. Jiao and G. Cao, *Phys. Stat. Sol. (a).* **2006,** 203, R22. **DOI:** 10.1002/pssa.200622038
29. P. Li, J.F. McDonald, T.M. Lu, *J. Appl. Phys.* **1992,** 71, 5596. **DOI:** 10.1063/1.350538
30. R. Kumar, M. Zulfequar, V.N. Singh, J.S. Tawale and T.D. Senguttuvan, *Journal of Alloys and compound.* **2012,** 541, 428. **DOI:** 10.1016/j.jallcom.2012.07.052
31. A. Ibarra, R. Heidinger, and J. Mola, *J. Nuclear Materials*. **1992,** 191, 530. **DOI:** 10.1016/S0022-3115(09)80101-3
32. A. K. Jonscher, *J. Mater. Sci.* **1981,** 16, 2037. **DOI:** 10.1007/BF00542364
33. L. Feng, M. Shen, and W. Cao, *J. Appl. Phys.* **2004,** 95, 6483. **DOI:** 10.1063/1.1728308
34. W. Cai, C. Fu, J. Gao and H. Chen, *J. Alloy and Compounds.* **2009,** 480, 870. **DOI:** 10.1016/j.jallcom.2009.02.049
35. C. A. Randall, N. Kim, J. P. Kucera, W. Cao, and T. R. Shrout, *J. Am. Ceram. Soc.* **1998,** 81, 677. **DOI:** 10.1111/j.1151-2916.1998.tb02389.x
36. T. M. Kamel, and G. D. With, *J. Euro. Ceram. Soc.* **2008,** 28, 851. **DOI:** 10.1016/j.jeurceramsoc.2007.08.010
37. T. B. Adams, D. C. Sinclair, and A. R. West, *Adv. Mater.* **2002,** 14, 1321. **DOI:** 10.1002/1521-4095(20020916)14:18<1321::AID-ADMA1321>3.0.CO;2-P
38. T. B. Adams, D. C. Sinclair, and A. R. West, *J. Am. Ceram. Soc.* **2006,** 89, 3129. **DOI:** 10.1111/j.1551-2916.2006.01184.x